Kinetic energy of He atoms in liquid ^{4}He-^{3}He mixtures

R. Senesi*
Istituto Nazionale per la Fisica della Materia, UdR Roma Tor Vergata, via della Ricerca Scientifica 1, 00133 Roma, Italy

C. Andreani
Dipartimento di Fisica, Università degli Studi di Roma Tor Vergata and Istituto Nazionale per la Fisica della Materia, via della Ricerca Scientifica 1, 00133 Roma, Italy

A. L. Fielding
Joint Department of Physics, Institute of Cancer Research and Royal Marsden Hospital, Downs Road, Sutton, Surrey SM2 5PT, United Kingdom

J. Mayers
Rutherford Appleton Laboratory, ISIS Facility, Chilton, Didcot, Oxon Ox11 0QX, United Kingdom

W. G. Stirling
European Synchrotron Radiation Facility, Boîte Postale 220, F-38043 Grenoble Cedex, France and Department of Physics, University of Liverpool, Liverpool L69 3BX, United Kingdom
(Received 7 July 2003; published 31 December 2003)

Deep inelastic neutron scattering measurements on liquid ^{3}He-^{4}He mixtures in the normal phase have been performed on the VESUVIO spectrometer at the ISIS pulsed neutron source at exchanged wave vectors of about $q \simeq 120.0$ Å^{-1}. The neutron Compton profiles $J(y)$ of the mixtures were measured along the $T = 1.96$ K isotherm for ^{3}He concentrations, x, ranging from 0.1 to 1.0 at saturated vapor pressures. Values of kinetic energies $\langle T \rangle$ of ^{3}He and ^{4}He atoms as a function of x, $\langle T \rangle(x)$, were extracted from the second moment of $J(y)$. The present determinations of $\langle T \rangle(x)$ confirm previous experimental findings for both isotopes and, in the case of ^{3}He, a substantial disagreement with theory is found. In particular $\langle T \rangle(x)$ for the ^{3}He atoms is found to be independent of concentration yielding a value $\langle T \rangle_3(x=0.1) \simeq 12$ K, much lower than the value suggested by the most recent theoretical estimates of approximately 19 K.

DOI: 10.1103/PhysRevB.68.214522 PACS number(s): 67.60.−g, 61.12.Ex

I. INTRODUCTION

The microscopic static and dynamic properties of liquid ^{4}He-^{3}He mixtures are characterized by the interplay between the Fermi (^{3}He) and Bose (^{4}He) statistics, the interatomic interaction, and the quantum-mechanical zero-point motion.[1,2] Moreover, the Pauli exclusion principle strongly influences the stability of the mixture.[1] Dilute solutions of ^{3}He atoms in liquid ^{4}He form a prototype quantum liquid as an example of an interacting boson-fermion mixture. Indeed the presence of ^{3}He affects the condensate fraction n_0, the superfluid fraction ρ_s/ρ_4 of ^{4}He, the individual momentum distributions $n(p)$, and the single-atom mean kinetic energy $\langle T \rangle$ of the two isotopes. In recent years, considerable efforts have been addressed to the understanding of microscopic static and dynamical properties in helium mixtures from both the experimental and the theoretical points of view.[2] Experimental deep inelastic neutron scattering (DINS) results have revealed significant and interesting discrepancies between theory and experiment as far as determination of the condensate fraction n_0 in the superfluid phase, mean kinetic energy $\langle T \rangle_3(x)$ of the lighter isotope, and momentum distributions are concerned.[3,4] Here, x is the concentration of ^{3}He in the mixture. We stress that a substantial agreement between theories exists for the values of n_0 and $\langle T \rangle_3(x)$ for low concentration mixtures.[5–9] These discrepancies have to be compared with the remarkable agreement found between theory and experiments for pure high density liquid and solid ^{3}He (Refs. 2,10–12) and pure fluid and solid ^{4}He (Refs. 13–16), respectively.

The single-atom mean kinetic energies $\langle T \rangle(x)$ reflect the localization of the two isotopes in the mixture and are influenced by the mixture concentration.[3,4,18,19] An important conclusion of DINS measurements in the concentration range $0.0 \leqslant x \leqslant 1.0$,[3,4] is that $\langle T \rangle_3(x)$ is essentially independent of x, indicating a local environment of the ^{3}He atoms in the mixtures similar to that of pure liquid ^{3}He. Ground state simulation techniques provide an insight into the local environment of ^{3}He and ^{4}He in liquid He mixtures and pure He liquids, allowing the evaluation of both partial radial distribution functions and single particle mean kinetic energies. In particular, simulation results for partial radial distribution functions $g_{\alpha,\beta}(r)$ in low concentration mixtures ($x \leqslant 0.1$) show two distinct features. The radial distribution function $g_{3,4}(r)$ and local density profile $\rho_{3,4}(r)$ are very similar to $g_{4,4}(r)$, $\rho_{4,4}(r)$, and to the pure ^{4}He radial distribution function.[9,17] The second feature is that $g_{3,4}(r)$ and $\rho_{3,4}(r)$ are markedly different from $g_{3,3}(r)$, $\rho_{3,3}(r)$ and from pure ^{3}He radial distribution function. These findings support a picture where the ^{3}He atoms experience a greater localization in the mixture with respect to pure ^{3}He, while the ^{4}He atoms show a microscopic structure similar to pure liquid ^{4}He. The first

feature accounts for the increased $\langle T\rangle_3$ values with respect to pure liquid ^{3}He.[5–7,9,18] In the case of ^{4}He, $\langle T\rangle_4$ is on the contrary similar to the pure liquid value for $x\rightarrow 0$, and a decrease of $\langle T\rangle_4$ with increasing concentration is found, in agreement with experimental DINS results. It has to be stressed that the similarity of $g_{3,4}(r)$ and $g_{4,4}(r)$ does not necessarily imply similar values of $\langle T\rangle_3$ and $\langle T\rangle_4$ in the mixture. Moreover, since the atomic density n in the mixtures is always larger than the atomic density of pure liquid ^{3}He, DINS results show that $\langle T\rangle_3$ is also independent of n; this, again, is in contrast with the widely-assessed density-dependence of mean kinetic energy of all quantum fluids and solids. As far as the experimental values of $\langle T\rangle_4(x)$ in the $0.0\leqslant x\leqslant 0.4$ range are concerned, these were found to be in agreement with microscopic calculations, resulting in a decrease of the kinetic energy of the ^{4}He atoms with increasing concentration.

These findings motivated the present measurements, which were performed over a wider concentration range, i.e., $x=0.00$, 0.10, 0.35, 0.65, 0.90, 1.00, and with an increased statistical accuracy than previous DINS experiments.[3,4] At present DINS is the only experimental technique which allows direct access to single-particle dynamical properties, such as the momentum distribution $n(\vec{p})$ and mean kinetic energy $\langle T\rangle$.[20] Experimentally this is achieved by exploiting the large values of wave vector and energy transfers involved in neutron scattering with epithermal neutrons.[19] The scattering process is well described within the framework of the impulse approximation (IA). In the IA the dynamical structure factor $S(\vec{q},\omega)$, which determines the scattered intensity, is given by

$$S_{\mathrm{IA}}(\vec{q},\omega)=\int n(\vec{p})\,\delta\left(\omega-\frac{\hbar q^2}{2M}-\frac{\vec{q}\cdot\vec{p}}{M}\right)d\vec{p}, \qquad (1)$$

where M is the atomic mass of the struck nucleus. The scaling properties of the scattering law can be expressed in terms of a scaling function $J(y,\hat{q})=(\hbar q/M)S_{\mathrm{IA}}(\vec{q},\omega)$, where $y=(M/\hbar q)(\omega-\hbar q^2/2M)$ is the West scaling variable.[19,21] The function $J(y,\hat{q})$, often referred to as the neutron Compton profile (NCP) or longitudinal momentum distribution,[19,21] represents the probability density distribution of y, the atomic momentum component along the direction of momentum transfer $\hat{q}$. In the present case the dependence on the direction of the momentum transfer $\hat{q}$ will be omitted given the absence of preferred orientations in the liquid samples. The values for $\langle T\rangle$ are obtained by exploiting the second moment sum rule for $J(y)$:[13,21]

$$\int_{-\infty}^{\infty} y^2 J(y)\,dy=\sigma_y^2=\frac{2M}{3\hbar^2}\langle T\rangle, \qquad (2)$$

where σ_y is the standard deviation of $J(y)$. DINS spectra from a liquid ^{3}He-^{4}He mixture will then be composed of two distinct contributions, one corresponding to the ^{4}He NCP, $J(y_4)$ and, in a different region of the DINS spectra, one to the ^{3}He NCP, $J(y_3)$. The $J(y_{3,4})$ functions can be separately analyzed and from their lineshape properties the momentum distributions and mean kinetic energies can be determined.

II. EXPERIMENT

The DINS measurements were carried out on the VESUVIO instrument, an inverse-geometry spectrometer operating at the ISIS pulsed neutron source (Chilton, Didcot-UK).[22] On this instrument the NCP spectrum is reconstructed using the filter difference technique which consists of measuring the time of flight of the neutrons scattered by the sample; the final energy is selected by a resonant foil analyzer located between sample and detectors.[20] For the present experiment the 4.908 eV resonance of a ^{197}Au foil filter was chosen. The scattered neutrons were detected by 32 glass scintillators (^{6}Li-enriched fixed-angle elements) placed over an angular range $115°<2\theta<144°$, yielding average wave vector transfers of $q\simeq 128$ and 116 Å^{-1} for ^{3}He and ^{4}He, respectively. These large values of wave vector transfers ensured that deviations from the IA, generally described in terms of the final state effects (FSE) (Ref. 13) were negligible and did not affect significantly the recoil peak shapes.[10,23] The corresponding average energy transfers accessed were $\hbar\omega\simeq 11$ and 7 eV for ^{3}He and ^{4}He, respectively. For highly absorbing ^{3}He this energy yields a favorable ratio between the absorption and scattering cross section of about 30.[10]

The experiment has been performed along the 1.96 K isotherm. Known amounts of gaseous ^{3}He and ^{4}He were first mixed in a reservoir at $T=293$ K. Six mixtures were prepared, for different ^{3}He concentrations, namely, $x=1.00$, 0.90,0.65,0.35,0.10,0.00. The mixtures were then allowed to condense into the sample cell to the homogeneous liquid phase at $T=1.96$ K. Special attention was paid to ensure that the liquid samples were in saturated vapor pressure conditions (SVP); this was achieved by measuring the vapor pressure of the samples on the top of the sample cell by a Baratron pressure transducer. The liquid samples were contained in a square flat aluminum cell (6 cm width, 6 cm height, 0.5 cm thickness) placed in a liquid helium flow cryostat; the sample temperatures were recorded by two Ge resistance thermometers located at the upper and lower ends of the sample cell, resulting in an average temperature $T=1.96$ K ± 0.01 K throughout the measurements. Experimental values of vapor pressure for each mixture composition x were found to be in agreement with SVP data in the literature.[24] For each composition DINS spectra were recorded for runs lasting about 24 h. The time-of-flight spectra were and normalized to the monitor counts by using standard routines available on VESUVIO.[20] In Fig. 1 a typical time of flight spectrum as recorded from a single detector for the $x=0.35$ mixture is displayed.

From this figure, one can note that the recoil peaks from the two different atomic masses occur at well separated positions in the time of flight spectrum. This is the case for the whole set of data in the angular range explored. Due to the high values of wave vector transfer accessed, the recoil peaks can be analyzed in wave vector spaces, i.e., $y_3=(M_3/\hbar q)(\omega-\hbar q^2/2M_3)$ and $y_4=(M_4/\hbar q)(\omega-\hbar q^2/2M_4)$ for ^{3}He and ^{4}He, respectively. The fixed-angle experi-

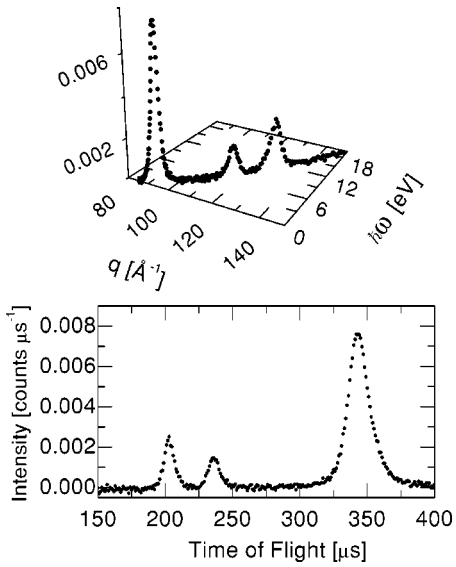

FIG. 1. Bottom: time of flight DINS spectrum from the $x=0.35$ mixture for a single detector at the scattering angle $2\theta=135°$. The ^{3}He and ^{4}He signals occur at approximately 205 and 240 μs, respectively; the sample cell signal is located at about 340 μs. Top: wave vector and energy transfer range accessed in the bottom spectrum.

mental resolution $R_l(y_{3,4})$, where l is the lth fixed-angle detector element, was determined for each detector through a standard VESUVIO experimental calibration using a lead sample. The $R_l(y_{3,4})$ as in previous measurements on ^{3}He (Refs. 10,25) and ^{4}He,[26] is well described by a Voigt function, whose parameters are $\sigma(y_3)=0.847$ Å^{-1}, $(\Gamma/2)(y_3)=1.371$ Å^{-1} and $\sigma(y_4)=0.839$ Å^{-1}, $(\Gamma/2)(y_4)=1.740$ Å^{-1}, where $\sigma(y)$ is the standard deviation of the Gaussian component and $(\Gamma/2)(y)$ is the half width at half maximum of the Lorentzian component. A parallel procedure has also been setup using Monte Carlo neutron transport simulation codes for the VESUVIO spectrometer[25,27,28] in order to simulate the complete moderator-sample-detector neutron transport, including multiple neutron scattering and energy dependent neutron absorption. This procedure provided simulated DINS measurements, a simulated resolution function $R_l(y)$, which agreed with both experimental data and experimentally calibrated $R_l(y)$.[25,27,28] This ensured the reliability of the current calibration procedure, and also allows the observed $J_{3,4}(y)$ to be described by a convolution of the longitudinal momentum distribution and the instrumental resolution function.[27]

Absorption and multiple scattering correction. The effects of the ^{3}He neutron absorption on the measured scattering from the liquid mixtures have been examined in detail, using both an analytical approach as well as a deterministic Monte Carlo simulation procedure. In ^{3}He the neutron absorption cross section is energy-dependent with the typical 1/v variation, with a value of 5333 b for 25 meV neutrons.[29] The incident energy range covered by the measured ^{4}He and ^{3}He recoil peaks were 9–15 and 13–20 eV, respectively (using Au absorption filters). Although the absorption cross section

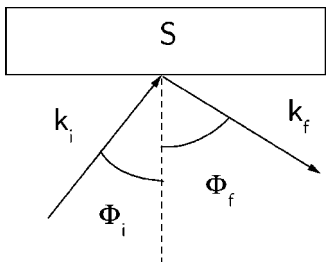

FIG. 2. Schematic diagram of the scattering geometry for analytical absorption corrections. S is the slab-shaped absorbing sample. $\Phi_{i,f}$ and $k_{i,f}$ are the angle of incidence (scattering) with respect to the normal to the sample, and initial (final) neutron wave vectors. Note that for the present case $\Phi_i=0$.

of ^{3}He has a relatively smooth variation in these ranges, we analyzed in detail the effects on the measured neutron Compton profiles. An approach for the analytic correction of absorption in strongly absorbing media was first proposed by Sears.[30] The double-differential scattering cross section is calculated by evaluating the distribution of scattered neutrons from a sample of finite size, with the quantities $S(q,\omega)$, the scattering function, and $\Sigma(k)$, the total cross section per unit volume for a neutron with wave vector k, occurring as parameters of the Boltzmann equation in the neutron transport theory.[31] In the ^{3}He case

$$\Sigma(k)=\Sigma_a(k)+\Sigma_s(k)\simeq\Sigma_a(k)\gg\Sigma_s(k), \tag{3}$$

where $\Sigma_a(k)$ and $\Sigma_s(k)$ are the absorption and scattering cross sections per unit volume; the beam attenuation due to multiple scattering is also found to be negligible, since the ratio of double to single scattering is of the order of $\Sigma_s(k)/2\Sigma(k)$.[31] In the case of a slab shaped sample and backscattering geometry, as shown in Fig. 2, the double-differential cross section for single scattering is given by

$$\frac{d^2\sigma}{d\Omega dE_f}=\left[\frac{A}{\Sigma(k_i)\sec(\Phi_i)+\Sigma(k_f)\sec(\Phi_f)}\right]n_3\sigma\frac{k_f}{4\pi k_i}S(q,\omega), \tag{4}$$

where A is the surface area of the sample, n_3 is the ^{3}He atomic number density, and σ is the atomic scattering cross section. The wave vector dependence of $\Sigma_a(k)$ is expressed by $\Sigma_a(k)=n_3\sigma_a(k)=n_3(4\pi/k)b_c''$ where b_c'' is the imaginary part of the coherent scattering length.[31,32]

Experimental time of flight spectra from different fixed-angle detectors have been transformed into y space and described in terms of the fixed-angle neutron Compton profiles $J_l(y)$ using standard VESUVIO procedures—details of the transformation of time of flight spectra in fixed-angle neutron Compton profiles are accurately described in Refs. 20, 33—in order to correct for the incident-wave-vector-dependent absorption an analytical correction has been applied to the y-transformed data

$$J(y)_{l,\mathrm{corr}} = J(y)_l \frac{x}{x\sigma_3 + (1-x)\sigma_4}\left[\sigma_a(k_f) + \sigma_a(k_i)\frac{k_i^2}{k_f^2 \cos\Phi_f}\right], \tag{5}$$

where $\sigma_a(k)$ is the wave-vector-dependent absorption of ^{3}He, and σ_3 and σ_4 are the scattering cross section for ^{3}He and ^{4}He, respectively. In the case of inverse-geometry spectrometers such as VESUVIO, the final wave vector is constant, and for a fixed angle spectrum, Eq. (5) assumes the form

$$J(y)_{l,\mathrm{corr}} = J_l(y)[A + Bk_i], \tag{6}$$

where A and B are constants depending on the scattering angle and the concentration x; finally, due the zero-order sum rule for $J(y)$, $J(y)_{l,\mathrm{corr}}$ (the suffix ''corr'' is then omitted in the next sections) have been normalized to unity.[30] The concentration dependent factor was first proposed by Hilton *et al.*[34] and is particularly valid under the current experimental conditions of large wavevector and energy transfers, where cross correlation between ^{3}He and ^{4}He cross sections are negligible. As a complementary procedure the Monte Carlo neutron transport code DINSMS (Ref. 28) has been also employed to evaluate multiple scattering contributions and to test the analytical absorption corrections in the mixtures. In particular this code accounts for the energy dependent absorption of the mixtures employing the following expression:

$$n[x\sigma_3 + (1-x)\sigma_4]e^{-n[x(\sigma_3+\sigma_a)+(1-x)\sigma_4]t}dt \tag{7}$$

which represents the probability that a neutron traveling along the $\hat{t}$ direction within the slab-shaped sample will scatter between t and $t+dt$. As expected, the ratio of double to single scattering intensities varied between 1.2% for the $x=0.1$ mixture and 0.1% for the $x=0.9$ mixture, in agreement with theoretical predictions.[30,31] Therefore multiple scattering corrections were neglected. Moreover, by comparing the ratio of simulated data in momentum space with and without absorption contributions included, the analytical correction factor [Eq. (5)] was recovered. An example of a correction factor, as derived from simulations for a $x=0.35$ mixture for a scattering angle of 135° is presented in Fig. 3.

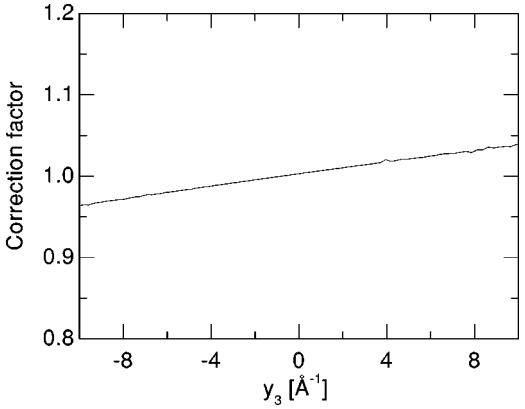

FIG. 3. Correction factor derived from the ratio of simulated data with and without absorption contributions.

III. DATA ANALYSIS AND RESULTS

The experimental spectra for each mixture composition were converted to ^{3}He and ^{4}He momentum space. Following this procedure a single function, $J(y)$, averaged over all the 32 detectors was derived for each isotope and for each composition.

The NCP were analyzed by simultaneously fitting the two recoil peaks appearing in $J(y_3)[J(y_4)]$. The component centered at $y=0$ in $J(y)$ was fitted by a model function $M(y)$ broadened by the instrumental resolution. The other component, centered at negative (^{4}He) or positive (^{3}He) y values were fitted using a Voigt function. The model function $M(y)$ used to describe the longitudinal momentum distribution was of the form

$$M(y) = \frac{e^{-y^2/2\sigma^2}}{\sqrt{2\pi\sigma^2}}\left[\sum_{n=2l}^{\infty} d_n H_n\left(\frac{y}{\sqrt{2\sigma^2}}\right)\right], \tag{8}$$

where $H_n(y/\sqrt{2\sigma^2})$ is the nth Hermite polynomial, and σ and d_n are fitting parameters; this functional form was applied by Sears[35] for the analysis of neutron scattering from pure liquid ^{4}He, and a generalized form, including angular dependencies, is currently used for momentum distribution spectroscopy in hydrogen containing systems on the VESUVIO spectrometer.[36] We used $d_0=1$ and $d_2=0$, in order that $M(y)$ satisfies the following sum rules:

$$\int_{-\infty}^{\infty} M(y)dy = 1, \tag{9}$$

$$\int_{-\infty}^{\infty} M(y)y^2 dy = \sigma^2 = \sigma_y^2. \tag{10}$$

In the present case orders up to $H_4(y/\sqrt{2\sigma^2})$ were employed. The inclusion of higher order polynomials did not result in significant improvements of the fits. As an example, in Fig. 4 the $J(y_3)$ function for three different compositions is presented, together with the fitted line shapes. The results for the determination of the mean kinetic energies for the two isotopes and the six mixture compositions are reported in Table I, and are shown in Fig. 5, in comparison with previous experiments and several theoretical predictions.

The present results extend the range of concentration x with respect to previous DINS measurements, with improved statistical accuracy. The ^{4}He kinetic energy is found to decrease with concentration, while the ^{3}He kinetic energy does not depend appreciably on the concentration.

IV. DISCUSSION AND CONCLUSIONS

The results of the present experiment show that the kinetic energy of ^{4}He atoms is strongly affected by the addition of ^{3}He; this is expected from density and quantum statistics arguments. A remarkable agreement with previous measurements and recent theories is found, with slight discrepancies with respect to finite temperature method

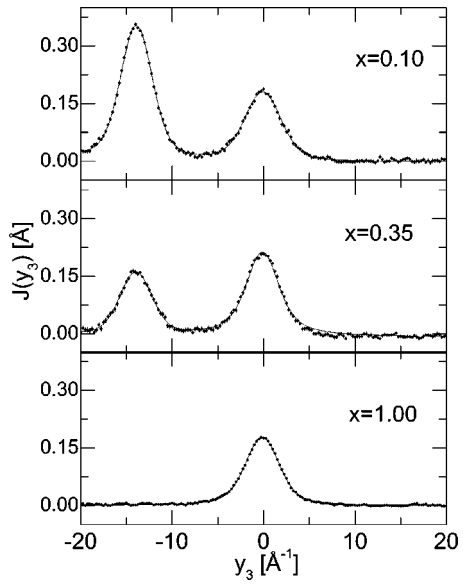

FIG. 4. $J(y_3)$ for the $x=0.10$, 0.35, and 1.00 mixtures (solid circles). The peak centered at negative values of momentum corresponds to the ^{4}He peak, centered at lower recoil energy. The solid lines are the fits to the neutron Compton profiles.

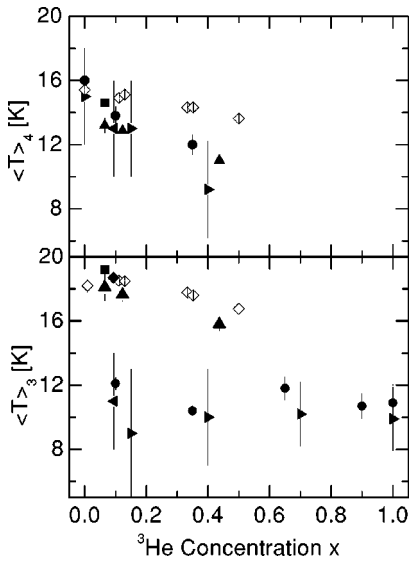

FIG. 5. Single-particle kinetic energies for ^{3}He (lower panel, solid circles) and ^{4}He (upper panel, solid circles), respectively, for the six mixtures. DINS experimental results from Azuah *et al.* (Ref. 3), right triangles. DINS experimental results from Wang *et al.* (Ref. 4), left triangles. Variational calculations at zero temperature for $x=0.066$ from Boronat *et al.* (Ref. 5), solid squares. Restricted path integral Monte Carlo calculations at $T=2$ K from Boninsegni *et al.* (Ref. 7), open diamonds. Variational Monte Carlo calculations at zero temperature from Lee *et al.* (Ref. 8), solid triangles. Restricted path integral Monte Carlo calculations at $T=2$ K from Boninsegni *et al.* (Ref. 9), solid diamond.

calculations.[7] On the other hand, the kinetic energy of the ^{3}He atoms appears unaffected by the presence of the higher density boson fluid, which seems to promote ^{3}He delocalization. It is illustrative to compare the $J(y_3)$ spectra for the $x=0.10$ mixture and for the pure ^{3}He fluid, as shown in Fig. 6, there is no substantial broadening of $J(y_3)$ on going from the pure liquid to the low-concentration mixture.

We stress that in several papers[5–7] the discrepancies between experiments and theories on the determinations of $\langle T\rangle_3$ have been attributed to high-energy tails in the dynamic structure factors, resulting in exponential-like tails in the momentum distributions, which could be masked by background noise, or are not accounted for using inadequate model functions for $J(y_3)$.[5–7] We point out, however, that since the high-energy tails are due to the repulsive part of the interatomic potential, they are present in the momentum distribution of the ^{4}He component as well. This is well illustrated by Fig. 6 of Ref. 5, where the momentum distributions of ^{3}He and ^{4}He in an $x=0.066$ mixture have practically the same high-momentum tails. The background noise is the same for the two isotopes in the same measurement, while the spectrometer resolution narrows on going from variables y_4 to y_3 in the same spectra; therefore one would expect an increased sensitivity to the detection of the high-momentum tails in $J(y_3)$. To test this hypothesis we simulated a measurement of $J(y_3)$ for an $x=0.066$ mixture in the experimental configuration of the present measurements. The momentum distribution published in Ref. 5, $n^{(3)}(k)$ of ^{3}He for the $x=0.066$ mixture at zero temperature was converted to $J(y_3)$ using the general result[19]

TABLE I. Single-particle kinetic energies for ^{3}He and ^{4}He, respectively, for the six mixtures. The density of the mixtures is also reported; density values were derived extrapolating the data from Table VI of Ref. 38 to $T=1.96$ K. Note that due to the very small intensities of the ^{4}He recoil peaks for the $x=0.65$ and the $x=0.90$ mixtures it was not possible to reliably determine $\langle T\rangle_4$.

x	n(nm^{-3})	$\langle T\rangle_3$ (K)	$\langle T\rangle_4$ (K)
0.00	21.87		16.0±0.5
0.10	21.40	12.1±0.4	13.8±0.6
0.35	19.94	10.4±0.3	12.0±0.6
0.65	18.22	11.8±0.7	
0.90	16.27	10.7±0.8	
1.00	15.44	10.9±0.4	

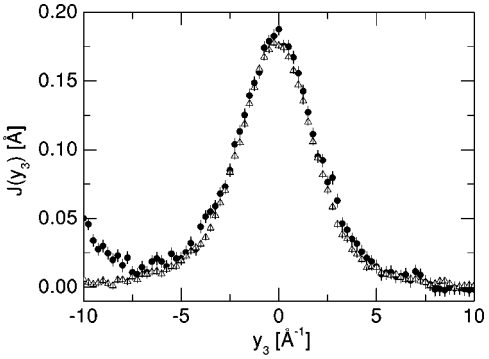

FIG. 6. $J(y_3)$ for the $x=0.10$ mixture, full circles and pure ^{3}He liquid ($x=1.00$), open triangles.

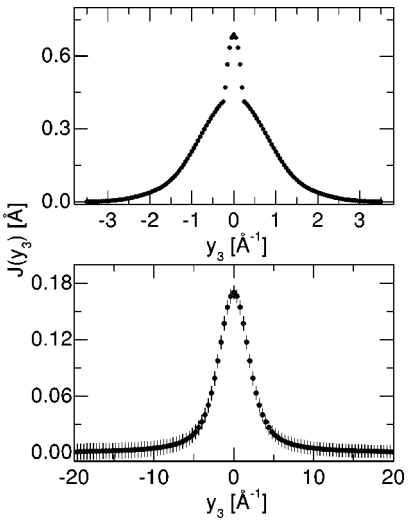

FIG. 7. Simulated $J(y_3)$ for a $x=0.066$ mixture. Upper panel, input Neutron Compton Profile derived from Ref. 5; lower panel, the resulting $J(y_3)$ after the simulation with the DINSMS code.

$$J(y)=\frac{1}{2\pi}\int_{|y|}^{\infty} dk\, k\, n(k). \tag{11}$$

This function shows pronounced high-momentum contributions due to the depletion of the Fermi sphere, the Fermi wave vector being $k_f=0.347$ Å^{-1}. The kinetic energy value, obtained from the second moment of the reconstructed $J(y_3)$ was $\langle T\rangle_3=18.2$ K. The function was used as input for the DINSMS code, which was run for a scattering angle of 135°. The input $J(y_3)$ and the simulated experiment are reported in Fig. 7.

The simulated spectrum was fitted by the convolution of a Voigt function, representing the spectrometer resolution, and two model functions: a simple Gaussian and the Gauss-Hermite expansion introduced above (Sec. III) with orders up to $H_8(y/\sqrt{2\sigma^2})$. The use of a single Gaussian resulted in $\langle T\rangle_3=16.7\pm0.4$ K, while the use of the Gauss-Hermite expansion resulted in $\langle T\rangle_3=17.0\pm0.4$ K. This indicates that the experimentally determined kinetic energies of ^{3}He are altered by less than 2.5 K, ruling out a strong effect of the high-momentum tails on the determination of kinetic energies.

A second test was performed to compare self-consistently the datasets available from the present measurements. The pure ^{3}He liquid data ($x=1.00$) were used as the calibration measurement, and $J(y_3)$ was modeled to have the functional form reported in Ref. 39, corresponding to a Fermi-like momentum distribution with a discontinuity at the Fermi momentum and high-momentum exponential tails; the resulting kinetic energy was $\langle T\rangle_3=11.7$ K, a value close to the theoretical predictions.[11] This function was convoluted with a Voigt function, an ''effective'' resolution to be determined from the fit to the pure liquid data. The resulting Voigt function had the following parameters $\sigma(y_3)=1.262$ Å^{-1}, $(\Gamma/2)(y_3)=0.9173$ Å^{-1}. This ''effective'' resolution was employed to fit the $x=0.1$ data, and the resulting kinetic energy was $\langle T\rangle_3=10.47\pm0.6$ K, confirming that no increase in kinetic energy, even in low-concentration mixtures, is indicated in the DINS experiments.

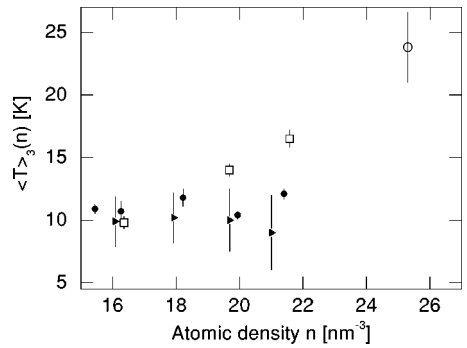

FIG. 8. $\langle T\rangle_3(n)$ for ^{3}He-^{4}He liquid mixtures and pure ^{3}He liquid; present measurements on the mixtures, solid circles; DINS experimental results from Azuah *et al.* (Ref. 3), on the mixtures, right triangles; pure liquid ^{3}He from Dimeo *et al.* (Ref. 37), open squares; high density pure liquid ^{3}He from Senesi *et al.* (Ref. 10), open circle.

This picture suggests that the local environment of the ^{3}He atoms remains unchanged in saturated vapor pressure liquid mixtures. Within the same picture, the $\langle T\rangle_3(x)$ behavior results also in a $\langle T\rangle_3(n)$ behavior, where n is the total atomic density, which differs radically from the widely assessed atomic-density dependence of kinetic energy of all quantum fluids and solids. Figure 8 shows the $\langle T\rangle_3(n)$ behavior of the mixtures, as compared to $\langle T\rangle_3(n)$ of the pure liquid.[10,37] The atomic density in the mixture is higher than in pure liquid ^{3}He in equilibrium, and increases up to $n=21.87$ nm^{-3} for $x=0$, upon adding ^{4}He.[38] A statistically significant departure from the density dependence observed in the pure fluid appears for $n\geqslant 19$ nm^{-3}. However, we stress that in this case the simultaneous changes of density and concentration prevent a thorough picture of the density and concentration dependence of $\langle T\rangle_3$. Systematic studies in several (concentration, pressure, temperature) thermodynamic states not previously investigated both experimentally and theoretically are certainly needed on the experimental and theoretical sides. For example, $\langle T\rangle_3(n)$ measurements on mixtures at fixed concentration (fixed concentration and increased pressure and density) would test whether the density dependence is recovered upon approaching and crossing the liquid-solid transition. However, previous and present results show unambiguously a behavior of $\langle T\rangle_3$ in the mixture which is not density dependent as for other quantum fluids and is not reproduced by any simulation studies.

The interpretation of these results is far from obvious. Two independent measurements[3,4] and the present work, have shown unequivocally that the ^{3}He kinetic energy in the mixtures is essentially independent on concentration and density. Further, we have shown that high-energy tails cannot explain this surprising result. Given the fact that a remarkable agreement between experiment and theory has been found for the pure helium liquids, we hope that our work

stimulates further theoretical and experimental effort. From the experimental point of view, we can envisage that high-resolution and high statistical quality data over an extended range of temperatures, compositions, and densities, can be obtained employing novel chopper and resonance filter spectrometers at pulsed neutron sources. However, the understanding of these results remains a challenge to conventional theories of liquid isotopic helium mixtures.

ACKNOWLEDGMENTS

This research has been supported by the VESUVIO project (EU Contract No. ERBFMGECT980142). R.S. kindly acknowledges J. Boronat, F. Mazzanti, and A. Polls for stimulating discussions. The authors acknowledge the ISIS User Support Group for the valuable technical support during experimental measurements.

*Electronic address: roberto.senesi@roma2.infn.it

[1] E. Krotscheck and M. Saarela, Phys. Rep. **232**, 1 (1993).
[2] E.R. Dobbs, *Helium Three* (Oxford University Press, Oxford, 2000).
[3] R.T. Azuah, W.G. Stirling, J. Mayers, I.F. Bailey, and P.E. Sokol, Phys. Rev. B **51**, 6780 (1995).
[4] Y. Wang and P.E. Sokol, Phys. Rev. Lett. **72**, 1040 (1994).
[5] J. Boronat, A. Polls, and A. Fabrocini, Phys. Rev. B **56**, 11 854 (1997).
[6] F. Mazzanti, A. Polls, and J. Boronat, Phys. Rev. B **63**, 054521 (2001).
[7] M. Boninsegni and S. Moroni, Phys. Rev. Lett. **78**, 1727 (1997).
[8] W.K. Lee and B. Goodman, Phys. Rev. B **24**, 2515 (1981).
[9] M. Boninsegni and D.M. Ceperley, Phys. Rev. Lett. **74**, 2288 (1995).
[10] R. Senesi, C. Andreani, D. Colognesi, A. Cunsolo, and M. Nardone, Phys. Rev. Lett. **86**, 4584 (2001).
[11] J. Casulleras and J. Boronat, Phys. Rev. Lett. **84**, 3121 (2000).
[12] S. Moroni, F. Pederiva, S. Fantoni, and M. Boninsegni, Phys. Rev. Lett. **84**, 2650 (2000).
[13] H.R. Glyde, *Excitations in Liquid and Solid Helium* (Clarendon Press, Oxford, 1994).
[14] H.R. Glyde, R.T. Azuah, and W.G. Stirling, Phys. Rev. B **62**, 14 337 (2000).
[15] U. Bafile, M. Zoppi, F. Barocchi, R. Magli, and J. Mayers, Phys. Rev. Lett. **75**, 1957 (1995).
[16] D.M. Ceperley, R.O. Simmons, and R.C. Blasdell, Phys. Rev. Lett. **77**, 115 (1996).
[17] A. Fabrocini, L. Vichi, F. Mazzanti, and A. Polls, Phys. Rev. B **54**, 10 035 (1996).
[18] J. Boronat and J. Casulleras, Phys. Rev. B **59**, 8844 (1999).
[19] *Momentum Distributions*, edited by R.N. Silver and P.E. Sokol (Plenum Press, New York, 1989).
[20] A.C. Evans, J. Mayers, D.N. Timms, and M.J. Cooper, Z. Naturforsch. A: Phys. Sci. **A48**, 425 (1993).
[21] G.I. Watson, J. Phys.: Condens. Matter **8**, 5955 (1996).
[22] R. Senesi, C. Andreani, Z. Bowden, D. Colognesi, E. Degiorgi, A.L. Fielding, J. Mayers, M. Nardone, J. Norris, M. Praitano, N.J. Rhodes, W.G. Stirling, J. Tomkinson, and C. Uden, Physica B **276–278**, 200 (2000).
[23] A.S. Rinat, M.F. Taragin, F. Mazzanti, and A. Polls, Phys. Rev. B **57**, 5347 (1998); K.H. Andersen, W.G. Stirling, and H.R. Glyde, *ibid.* **56**, 8978 (1997).
[24] S.G. Sydoriak and T.R. Roberts, Phys. Rev. **118**, 901 (1960).
[25] R. Senesi, C. Andreani, and D. Colognesi, J. Low Temp. Phys. **126**, 57 (2002).
[26] D. Colognesi, C. Andreani, and R. Senesi, Europhys. Lett. **50**, 202 (2000).
[27] C. Andreani, D. Colognesi, E. Degiorgi, A. Filabozzi, M. Nardone, E. Pace, A. Pietropaolo, and R. Senesi, Nucl. Instrum. Methods Phys. Res. A **497**, 535 (2003).
[28] J. Mayers, A.L. Fielding, and R. Senesi, Nucl. Instrum. Methods Phys. Res. A **481**, 454 (2002).
[29] S.F. Mughabghab, M. Divadeenam, and N.E. Holden, *Neutron Cross-sections* (Academic Press, New York, 1981), Vol. 1.
[30] V.F. Sears, J. Phys. C **9**, 409 (1976).
[31] V.F. Sears, Adv. Phys. **24**, 1 (1975).
[32] V.F. Sears and F.C. Khanna, Phys. Lett. **56B**, 1 (1975).
[33] G. Baciocco, C. Andreani, and J. Mayers, Nucl. Instrum. Methods Phys. Res. A **276**, 297 (1989); G. Baciocco, C. Andreani, and J. Mayers, in *Momentum Distributions*, edited by R.N. Silver and P.E. Sokol (Plenum Press, New York, 1989); A.D. Taylor (unpublished).
[34] P.A. Hilton, R. Scherm, and W.G. Stirling, J. Low Temp. Phys. **27**, 851 (1977).
[35] V.F. Sears, Phys. Rev. **185**, 200 (1969).
[36] G.F. Reiter, J. Mayers, and P. Platzman, Phys. Rev. Lett. **89**, 135505 (2002), and references therein.
[37] R. Dimeo, P.E. Sokol, R.T. Azuah, S.M. Bennington, W.G. Stirling, and K. Guckelsberger, Physica B **241**, 952 (1994).
[38] H.A. Kierstead, J. Low Temp. Phys. **24**, 497 (1976).
[39] R.T. Azuah, W.G. Stirling, K. Guckelsberger, R. Scherm, S.M. Bennington, M.L. Yates, and A.D. Taylor, J. Low Temp. Phys. **101**, 951 (1995).